Original Paper

Journal of Biomedical Science

J Biomed Sci 1999;6:115–120

Received: August 2, 1998
Accepted: September 14, 1998

Isolation of Full-Length cDNA and Chromosomal Localization of Human NF-κB Modulator NEMO to Xq28

Dong-Yan Jin Kuan-Teh Jeang

Molecular Virology Section, Laboratory of Molecular Microbiology, National Institute of Allergy and Infectious Diseases, Bethesda, Md., USA

Key Words

NF-κB · IκB · IκB kinase · NEMO · HTLV-1 Tax · Human chromosome Xq28

Abstract

NEMO is an essential component of the IκB kinase complex. Others have shown that expression of mouse NEMO can complement the lack of responsiveness to NF-κB stimuli in two NEMO-deficient cell lines. Here we report the isolation of a full-length human NEMO cDNA. Virtual translation of human NEMO cDNA predicts a 48-kD coiled-coil protein which shares 87.9% identity and 90.5% similarity with the mouse homolog. By sequence alignment, we mapped the human NEMO gene to chromosome Xq28. We note that the NEMO and the G6PD (glucose-6-phosphate dehydrogenase) loci are arranged in a head-to-head orientation separated by no more than 800 bp. This map location is further supported by the sequence of an alternatively spliced variant of human NEMO mRNA. Thus, human NEMO is an X-linked gene closely adjacent to the G6PD locus.

The transcription factor NF-κB regulates the expression of various cellular and viral genes. NF-κB plays important regulatory roles in immune and inflammatory responses, and in apoptosis. NF-κB exists ambiently in the cytoplasm via association with inhibitor protein IκB. Activation of NF-κB is induced by a wide variety of stimuli including cytokines, phorbol ester, bacterial lipopolysaccharide (LPS), and virus infection [1, 9].

One pathway of NF-κB activation involves site-specific phosphorylation and subsequent ubiquitination/degradation of IκB. The dissociation of IκB results in the unmasking of the NF-κB nuclear localization signal facilitating entry of protein into the nucleus. Thus, IκB phosphorylation represents a critical mechanism for regulation of nuclear NF-κB activity [1, 9, 13]. To date, at least two IκB kinases, IKK-1 and IKK-2, have been cloned and characterized [17, 22, 25, 36]. However, it has been suggested that these factors are components of a larger multiprotein complex [17, 20].

Recently, a novel component of the IκB kinase complex in mouse cells was identified by complementation cloning [34]. This dimeric protein, termed NEMO (NF-κB essential modulator), was found to associate directly with IKK-2. Expression of NEMO was shown to complement the lack of responsiveness to NF-κB stimuli in two

KARGER
Fax + 41 61 306 12 34
E-Mail karger@karger.ch
www.karger.com

Accessible online at:
http://BioMedNet.com/karger

Kuan-Teh Jeang
LMM/NIAID/NIH, Building 4, Room 306
9000 Rockville Pike
Bethesda, MD 20892-0460 (USA)
Tel. +1 301 496 6680, Fax +1 301 480 3686, E-Mail kj7e@nih.gov

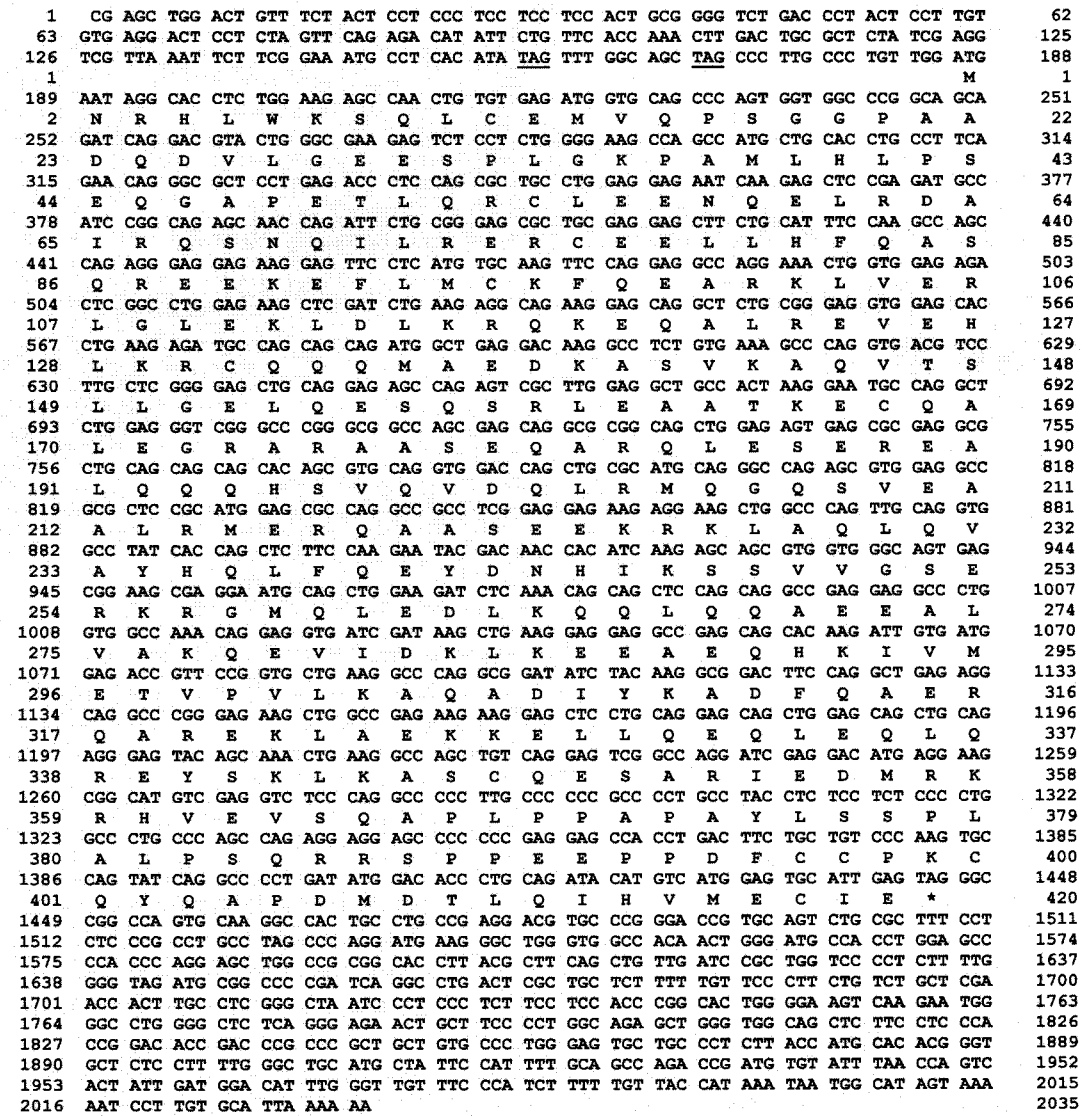

Fig. 1. The nucleotide and deduced amino acid sequences of human NEMO. Two in-frame stop codons upstream the translation initiation site are underlined. Presence of poly (A) tail at the 3′-terminus is not shown. The GenBank accession number for this nucleotide sequence is AF091453.

NEMO-defective cell lines, one of which was transformed by human T-cell leukemia virus type 1 (HTLV-1) oncoprotein Tax.

Previously, we have studied aspects of Tax-mediated transcription [11, 12, 30] and transformation [26, 29] in mammalian cells. In particular, we have identified cellular targets of Tax, including GPS2 [14], Int-6 [23], cytokeratin [32], Rb [24] and MAD1 [15, 16]. Tax has also been suggested by others to target components of the IκB kinase complex including MEKK-1 [35], NIK [8, 33], IKK-1 [5, 8, 33] and IKK-2 [5, 8, 33]. The characterization of mouse NEMO as a novel Tax target [34] prompted us to investigate its involvement in the interaction of Tax with the IκB kinase complex. As a first step, here we report the isolation of a full-length human NEMO cDNA and the chromosomal localization of this gene to Xq28, in close proximity to the locus of glucose-6-phosphate dehydrogenase (G6PD).

Materials and Methods

Molecular Cloning of Human NEMO

Standard procedures of molecular cloning were followed [27]. Full-length nucleotide and protein sequences of mouse NEMO were used to search the National Center for Biotechnology Information expressed sequence tag (EST) database dbEST (World Wide Web site: http://www.ncbi.nlm.nih.gov). Multiple overlapping EST clones were identified. To derive and confirm the 5′ sequences, rapid amplification of cDNA ends (RACE) was performed using a HeLa cell cDNA library. Genomic sequences were identified by screening the GenBank database. Double-stranded DNAs were sequenced on both strands using the dideoxy method.

Sequence Analysis

Nucleotide and peptide sequences were analyzed with the Wisconsin software package (Version 8.1, Genetics Computer Group, Inc.) and the CGG (Computational Computer Group, Sanger Center) genomic analysis tools. Similarity searching and comparison were performed by the BLAST and BESTFIT programs. COILS [19] and PAIRCOIL [2] algorithms were used to assist prediction of coiled coils in the NEMO protein. Predictions of RNA polymerase II promoter and transcriptional initiation sites were through the TSSG and TSSW server [31] (World Wide Web site: http://dot.imgen.bcm.tmc.edu:9331/gene-finder/gf.html).

Chromosomal Mapping

The nucleotide sequences (GenBank accession numbers L44140, X55448, X53815) of the YAC and cosmid clones previously mapped to human chromosome Xq28 were used for physical alignment of human NEMO. The flanking marker is G6PD [3, 4, 21].

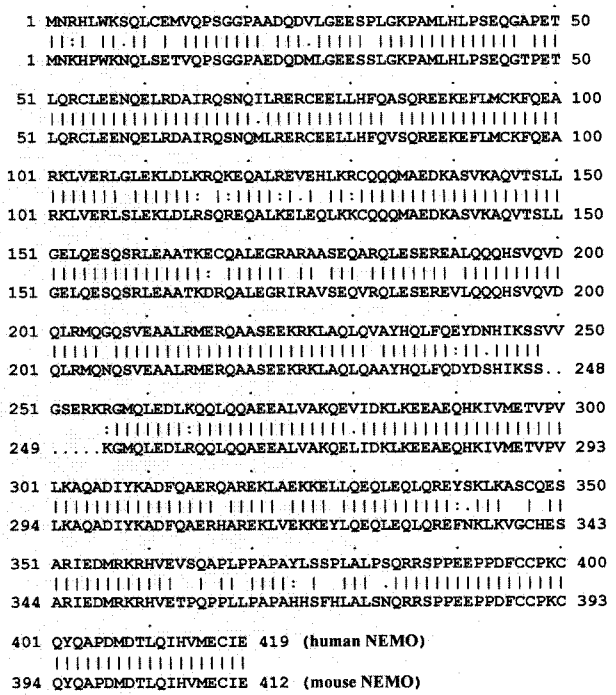

Fig. 2. Amino acid sequence alignment of human and mouse NEMO. Bars indicate identity and colons represent similarity. The alignment was generated by the BESTFIT program in the Wisconsin package.

Results and Discussion

Molecular Cloning of Human NEMO cDNA

A 2,035-bp full-length human NEMO cDNA was cloned and sequenced (fig. 1; GenBank AF091453). The presence of two in-frame stop codons (underlined in fig. 1) immediately upstream of the putative translation initiation codon supports a conclusion that the presented NEMO open reading frame (ORF) is likely to be complete. The human NEMO ORF contains 421 amino acid residues, with a predicted molecular size of 48 kD. We performed a homology search using the BLAST program. This revealed that human NEMO shares 87.9% identity and 90.5% similarity with its mouse homolog (fig. 2). In addition, NEMO is distantly related to a subgroup of coiled-coil proteins including FIP2 that interacts with adenovirus E3 14.7-kD protein [18] (GenBank AF061034, $P(N) = 4 \times 10^{-15}$), NuMA [6] (PIR S23647, $P(N) = 6 \times 10^{-7}$), centrosome-associated protein c-NAP1 [7] (GenBank AF049105, $P(N) = 1 \times 10^{-6}$), NIK (GenBank U88984, $P(N) = 5 \times 10^{-6}$), and KIAA0445 that interacts with Tax [28] [Jin and Jeang, unpubl. data] (GenBank AB007914, $P(N) = 2 \times 10^{-4}$).

Further analysis revealed that the coiled coils in NEMO encompass residues 51 to 353 (fig. 3). This coiled-coil domain of NEMO likely facilitates its protein-protein interaction with other factors including IKK-2. Based on this reasoning it would be of interest to investigate whether NEMO can also interact directly with adenovirus E3 14.7-kD protein, centrosomal proteins, NIK and Tax. In this regard, Tax has been reported to associate with IKK-1, IKK-2, NIK and MEKK-1 [5, 8, 33, 35]. Plausibly, Tax would cooperate with NEMO in the regulation of IκB and NF-κB.

Chromosomal Mapping of Human NEMO Gene

By sequence alignment, we identified three genomic clones that contain the 5′-noncoding sequence of the human NEMO cDNA. These are HSG6PDG (GenBank X53815), HSG6PDGEN (GenBank X55448), and HUMFLNG6PD (GenBank L44140). These three genomic fragments all co-localize to human chromosome

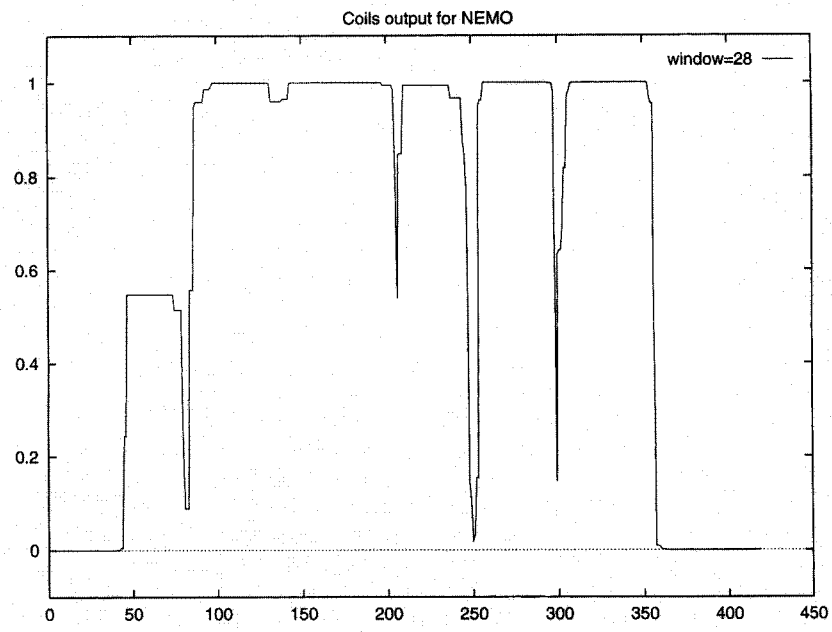

Fig. 3. Predicted coiled-coil structure in human NEMO. The x-axis represents residues in NEMO. The y-axis is the probability to form coiled coils. The plot was generated by the COILS program [19] using the MTIDK matrix. A 2.5-fold weighting was given to position *a* and *d*. Prediction by the PAIRCOIL program (2) yielded similar results.

Xq28 [3, 4, 21]. The deduced NEMO gene in the three clones was noted to be closely linked to the G6PD locus, but the orientations of the NEMO and G6PD genes are in opposing directions. Thus, NEMO maps to Xq28, in close contiguity to G6PD.

It cannot be formally excluded that our NEMO cDNA might be chimeric for two genes. While this occurrence is rare, it has been previously documented [10]. To address this concern, we searched for additional human NEMO cDNA clones. Another independent human NEMO cDNA (GenBank AI124572) was identified. The coding sequences of AF091453 and AI124572 are identical. However, the two 5′-noncoding regions were completely different in sequence. Interestingly, both 5′ untranslated sequences (AF091453 and AI124572) were intactly present adjacent to each other and separated by 170 nucleotides in the G6PD genomic clones HSG6PDG, HSG6PDGEN and HUMFLNG6PD (fig. 4). Thus, we reasoned that the two cDNAs likely represent alternatively spliced variants of the same human NEMO transcript. The AI124572 sequence provides further support to the deduced map location of human NEMO, which is separated from G6PD by less than 800 bp and is predicted to be transcribed in the opposing direction towards the telomere (fig. 4, 5). A prominent CpG island exists in the G6PD-NEMO region and the putative promoters for NEMO and G6PD are separated by 740 bp.

Chromosome Xq28 is a region of interest in human genetics (web site: http://www.ncbi.nlm.nih.gov/omim/). Several disease genes and fragile sites have been localized to Xq28 [4, 21]. The rate of crossovers in this region is relatively high [21]. The chromosomal mapping of NEMO to this location provides novel opportunities to study the physiologically regulated expression of this gene.

Acknowledgment

We thank Alicia Buckler-White for assistance in DNA sequencing and Hua Xiao, Vincenzo Giordano, and Karen Kibler for critically reading the manuscript.

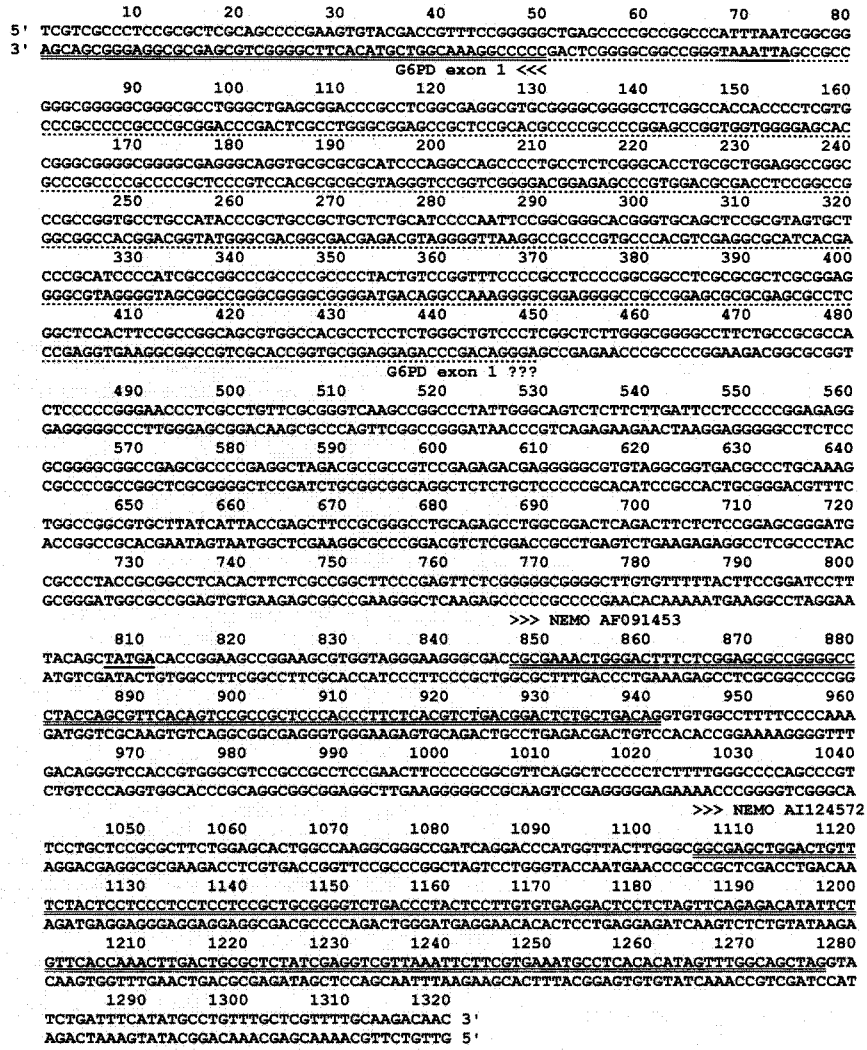

Fig. 4. Partial genomic sequences from the 5′ upstream region of the human NEMO and G6PD genes. Putative TATA boxes (positions 70 and 810) for G6PD and NEMO are underlined. Exon sequences are doubly underlined. The major transcription initiation site of G6PD was experimentally determined [21]. An alternative first exon for G6PD was separately predicted [3, 4] and is highlighted by dots.

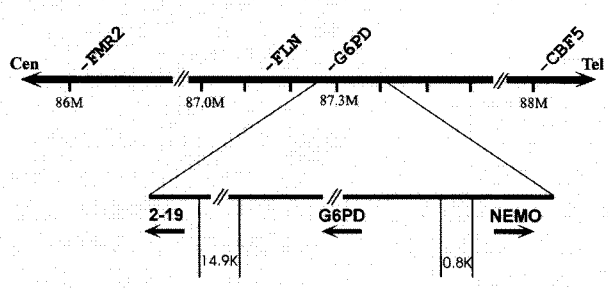

Fig. 5. Schematic delineation of human NEMO at Xq28. Positional numbering (in Mb) is anchored at the p telomere. Arrows underlying the genes indicate the orientation of transcription. Cen = Centromeric; Tel = Telomeric.

References

1 Baeuerle PA, Baltimore D. NF-κB: Ten years after. Cell 87:13–20;1996.

2 Berger B, Wilson DB, Wolf E, Tonchev T, Milla M, Kim PS. Predicting coiled coils by use of pairwise residue correlations. Proc Natl Acad Sci USA 92:8259–8263;1995.

3 Chen EY, Cheng A, Lee A, Kuang WJ, Hillier L, Green P, Schlessinger D, Ciccodicola A, D'Urso M. Sequence of human glucose-6-phosphate dehydrogenase cloned in plasmids and a yeast artificial chromosome. Genomics 10: 792–800;1991.

4 Chen EY, Zollo M, Mazzarella R, Ciccodicola A, Chen CN, Zuo L, Heiner C, Burough F, Repetto M, Schlessinger D, D'Urso M. Long-range sequence analysis in Xq28: Thirteen known and six candidate genes in 219.4 kb of high GC DNA between the RCP/GCP and G6PD loci. Hum Mol Genet 5:659–668;1996.

5 Chu ZL, DiDonato JA, Hawiger J, Ballard DW. The tax oncoprotein of human T-cell leukemia virus type 1 associates with and persistently activates IκB kinases containing IKKα and IKKβ. J Biol Chem 273:15891–15894; 1998.

6 Compton DA, Szilak I, Cleveland DW. Primary structure of NuMA, an intranuclear protein that defines a novel pathway for segregation of proteins at mitosis. J Cell Biol 116:1395–1408; 1992.

7 Fry AM, Mayor T, Meraldi P, Stierhof Y-D, Tanaka K, Nigg EA. C-Nap1, a novel centrosomal coiled-coil protein and candidate substrate of the cell cycle-regulated protein kinase Nek2. J Cell Biol 141:1563–1574;1998.

8 Geleziunas R, Ferrell S, Lin X, Mu Y, Cunningham ET Jr, Grant M, Connelly MA, Hambor JE, Marcu KB, Greene WC. Human T-cell leukemia virus type 1 Tax induction of NF-κB involves activation of the IκB kinase α (IKKα) and IKKβ cellular kinases. Mol Cell Biol 18: 5157–5165;1998.

9 Ghosh S, May MJ, Kopp EB. NF-κB and Rel proteins: Evolutionarily conserved mediators of immune responses. Ann Rev Immunol 16: 225–260;1998.

10 Jin D-Y, Lyu M-S, Kozak CA, Jeang K-T. Functions of 14-3-3 proteins. Nature 382:308; 1996.

11 Jin D-Y, Jeang K-T. HTLV-I Tax self-association in optimal trans-activation function. Nucl Acids Res 25:379–387;1997.

12 Jin D-Y, Jeang K-T. Transcriptional activation and self-association in yeast: Protein-protein dimerization as a pleiotropic mechanism of HTLV-1 Tax function. Leukemia 11:3–6; 1997.

13 Jin D-Y, Chae HZ, Rhee SG, Jeang K-T. Regulatory role for a novel human thioredoxin peroxidase in NF-κB activation. J Biol Chem 272: 30952–30961;1997.

14 Jin D-Y, Teramoto H, Giam C-Z, Chun RF, Gutkind JS, Jeang K-T. A human suppressor of c-Jun N-terminal kinase 1 activation by tumor necrosis factor α. J Biol Chem 272:25816–25823;1997.

15 Jin D-Y, Spencer F, Jeang K-T. Human T cell leukemia virus type I oncoprotein Tax targets the human mitotic checkpoint protein MAD1. Cell 93:81–91;1998.

16 Krishnan R, Goodman B, Jin D-Y, Jeang K-T, Collins C, Stetten G, Spencer F. Map location and gene structure of the Homo sapiens mitotic arrest deficient 2 (MAD2L1) gene at 4q27. Genomics 49:475–478;1998.

17 Lee FS, Peters RT, Dang LC, Maniatis T. MEKK1 activates both IκB kinase α and IκB kinase β. Proc Natl Acad Sci USA 95:9319–9324;1998.

18 Li Y, Kang J, Horwitz MS. Interaction of an adenovirus E3 14.7-kilodalton protein with a novel tumor necrosis factor α-inducible cellular protein containing leucine zipper domains. Mol Cell Biol 18:1601–1610;1998.

19 Lupas A, Van Dyke M, Stock J. Predicting coiled coils from protein sequences. Science 252:1162–1164;1991.

20 Maniatis T. Catalysis by a multiprotein IκB kinase complex. Science 278:818–819;1997.

21 Martini G, Toniolo D, Vulliamy T, Luzzatto L, Dono R, Viglietto G, Paonessa G, D'Urso M, Persico MG. Structural analysis of the X-linked gene encoding human glucose 6-phosphate dehydrogenase. EMBO J 5:1849–1855;1986.

22 Mercurio F, Zhu H, Murray BW, Shevchenko A, Bennett BL, Li JW, Young DB, Barbosa M, Mann M, Manning A, Rao A. IKK-1 and IKK-2: Cytokine-activated IκB kinases essential for NF-κB activation. Science 278:860–866;1997.

23 Neuveut C, Jin D-Y, Semmes OJ, Diella F, Callahan R, Jeang K-T. Divergent subcellular locations of HTLV-Tax and Int-6: A contrast between in vitro protein-protein binding and intracellular protein colocalization. J Biomed Sci 4:229–234;1997.

24 Neuveut C, Low KG, Maldarelli F, Schmitt I, Majone F, Grassmann R, Jeang K-T. Human T- cell leukemia virus type 1 Tax and cell cycle progression: Role of cyclin D-cdk and p110Rb. Mol Cell Biol 18:3620–3632;1998.

25 Regnier CH, Song HY, Gao X, Goeddel DV, Cao Z, Rothe M. Identification and characterization of an IκB kinase. Cell 90:373–383; 1997.

26 Rosin O, Koch C, Schmitt I, Semmes OJ, Jeang K-T, Grassmann R. A human T-cell leukemia virus Tax variant incapable of activating NF-κB retains its immortalizing potential for primary T-lymphocytes. J Biol Chem 273:6698–6703;1998.

27 Sambrook J, Fritch EF, Maniatis T: Molecular Cloning: A Laboratory Manual, ed 2. New York, Cold Spring Harbor Laboratory Press, 1989.

28 Seki N, Ohira M, Nagase T, Ishikawa K, Miyajima N, Nakajima D, Nomura N, Ohara O. Characterization of cDNA clones in size-fractionated cDNA libraries from human brain. DNA Res 4:345–349;1997.

29 Semmes OJ, Barret JF, Dang CV, Jeang K-T. Human T-cell leukemia virus type I tax masks c-Myc function through a cAMP-dependent pathway. J Biol Chem 271:9730–9738;1996.

30 Semmes OJ, Jeang K-T. Localization of human T-cell leukemia virus type 1 Tax to subnuclear compartments that overlap with interchromatin speckles. J Virol 70:6347–6357; 1996.

31 Solovyev VV, Salamov AA, Lawrence CB. Predicting internal exons by oligonucleotide composition and discriminant analysis of spliceable open reading frames. Nucl Acids Res 24:5156–5163;1994.

32 Trinh D, Jeang K-T, Semmes OJ. HTLV-I Tax and cytokeratin: Tax-expressing cells show morphological changes in keratin-containing cytoskeletal networks. J Biomed Sci 4:47–53; 1997.

33 Uhlik M, Good L, Xiao G, Harhaj EW, Zandi E, Karin M, Sun SC. NF-κB-inducing kinase and IκB kinase participate in human T-cell leukemia virus I tax-mediated NF-κB activation. J Biol Chem 273:21132–21136;1998.

34 Yamaoka S, Courtois G, Bessia C, Whiteside ST, Weil R, Agou F, Kirk HE, Kay RJ, Israel A. Complementation cloning of NEMO, a component of the IκB kinase complex essential for NF-κB activation. Cell 93:1231–1240;1998.

35 Yin MJ, Christerson LB, Yamamoto Y, Kwak YT, Xu S, Mercurio F, Barbosa M, Cobb MH, Gaynor RB. HTLV-I Tax protein binds to MEKK1 to stimulate IκB kinase activity and NF-κB activation. Cell 93:875–884;1998.

36 Zandi E, Chen Y, Karin M. Direct phosphorylation of IκB by IKKα and IKKβ: Discrimination between free and NF-κB-bound substrate. Science 281:1360–1363;1998.